

Design and experiment of the key components of the seeding monomer for high-speed corn no-till seeders

Yongliang Chen^{1,3}, Hairong Jing¹, Zhe Zhang¹, Yuhang Guo¹, Xiaofeng Ning^{1,2*}

(1. College of Engineering, Shenyang Agricultural University, Shenyang 110866, China;

2. Key Laboratory of Modern Horticultural Equipment, Ministry of Agriculture and Rural Affairs, Shenyang 110866, China;

3. Heilongjiang Dewo Technology Development Co., LTD, Harbin 150081, China)

Abstract: Aiming at the problems of uneven plant spacing, row spacing and sowing depth due to the collision of seeds with the tube wall or bouncing on the floor of the seed guide tube with the increase of operation speed of the current corn no-till planter, in this study, the high-speed seed belt technology was combined with the finger clip seed discharge device, a kind of high-speed no-till planter monomer was designed and installed in high-speed seed tube. At the same time, simulation analysis was made on the movement law of seeds in the seed guide tube when they fell from the finger clip seeder and the main structural parameters and the range of key parameters of the high-speed seed tube were determined. Through the prototype, the single-factor and quadratic orthogonal rotational combination test method, and the machine operating speed, the height of the high-speed seed tube and the seed guide angle were selected as the test factors in the seeding performance test. After parameter optimization, the optimal working parameters were determined: the machine forward speed was 12.18 km/h, the height of the high-speed seed tube from the ground was 42.22 mm, and the seed guide angle of the high-speed seed tube was 8.82°. The field test verified that under this parameter combination, the qualified-seeding index was 94.95%, the multiple-seeding index was 2.37%, and the missing-seeding index was 2.48%, showing stable working performance and satisfied the sowing and agronomic requirements of the no-till seeding operation.

Keywords: no-till planter, seeding monomer, high-speed seed tube, field test

DOI: [10.25165/ijabe.20231605.7687](https://doi.org/10.25165/ijabe.20231605.7687)

Citation: Chen Y L, Jing H R, Zhang Z, Guo Y H, Ning X F. Design and experiment of the key components of the seeding monomer for high-speed corn no-till seeders. *Int J Agric & Biol Eng*, 2023; 16(5): 95–103.

1 Introduction

Northeast China is one of the four major fertile black soil areas in the world and serves as an important agricultural product base for the country. However, over the years, the highly intensive and predatory development of black soil overused the black soil without nurturing, as a result, the black soil layer has become thinner and the organic matter content has decreased. Over the years, researchers have been working on the core issues of black soil conservation and have proposed several conservation tillage models. Conservation tillage can effectively reduce soil erosion and protect the ecological environment of farmland through less tillage and no-tillage, taking into account the sustainable development of agricultural ecological environment while obtaining economic benefits^[1]. A no-till planter is an important agricultural tool in the conservation tillage process^[2-5]. Compared with traditional seeders, the high-efficiency no-till planter differs mainly in the operating environment and the functions of working parts in entering soil^[6-10].

The most important functional component of the high-speed

seeder is seed metering device. At present stage, the seed metering device of high-speed corn seeder with technical advantages is mainly pneumatic seed metering device, including air suction type, air blowing type and air pressure type, among which the air suction type seed metering device is the most commonly used.

At present, the operating speed of no-till seeders has been improved while at the same time keeping the seeding spacing and sowing depth consistent without affecting the quality of seeding. The consistency between seeding spacing and sowing depth is an issue that needs to be solved urgently at present for no-till seeding machines^[11-13]. The uniform seed flow formed by the high-performance seed disperser currently in use can fall smoothly into the seed furrow, and this result largely depends on the structure of the seed guide^[14-16]. At present, the commonly used seed guide is made of plastic. The height and shape of the seed guide tube affect the uniformity of plant spacing and sowing depth, and its shape has gradually matured after years of upgrading^[17,18]. When seeds fall freely from the seed row, they will fall freely in the seed furrow on the ground through the common seed tube. During the process, they will collide and bounce in the seed guide tube. At the same time, the seeds will also bounce twice on the ground, affecting the accuracy of plant spacing and depth to a certain extent. When the seed speed is close to “zero speed seeding”, the influence of the seed guide tube on the index of sowing uniformity and the qualified index in grain spacing is small^[19-21]. When the operation speed of the no-till seeding machine is 8 km/h, the rotational speed of the seed tray reaches 44 r/min, the optimal working performance of the seed guide can be achieved to ensure uniform plant spacing and sowing depth. On the contrary, when the operating speed is higher than 8 km/h, rotational speed of seed tray is higher than 44 r/min, it is

Received date: 2022-05-19 **Accepted date:** 2023-10-13

Biographies: Yongliang Chen, MS candidate, research interest: no-tillage seeding technology and equipment, Email: 1093305025@qq.com; Hairong Jin, MS candidate, research interest: no-tillage seeding technology and equipment, Email: 1696118606@qq.com; Zhe Zhang, MS candidate, research interest: no-tillage seeding technology and equipment, Email: 1010082970@qq.com; Yuhang Guo, MS candidate, research interest: no-tillage seeding technology and equipment, Email: 2356400798@qq.com.

***Corresponding author:** Xiaofeng Ning, Associate Professor, research interest: intelligent agricultural machinery equipment. College of Engineering, Shenyang Agricultural University, 120 Dongling Road, Shenyang 110866, China, Tel: +86-13898155846, Email: ningxiaofeng123@syau.edu.cn.

impossible to achieve uniform plant spacing and sowing depth^[22-24].

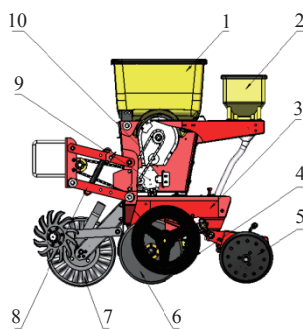
At present, foreign high-speed corn seeding technology begins to strengthen the research on stable migration technology. The key goal is to accelerate the motion of seeds from leaving the seed metering device to the seedbed, thus effectively control the angle and initial velocity of seed falling, so as to reduce the impact of collision on the actual planting position. From this perspective, there are not enough researches on the control of corn seed backward position in China, and there are rarely models used in practice. Therefore, it is very important to strengthen the research and application of precise corn seed positioning technology.

According to the requirement of efficient planting, in this study, a high-speed no-till planter monomer that combines the "high-speed seed belt technology" with the finger clip seeder of a no-till planter, and a new high-speed seed tube with trapezoidal tooth timing belt were designed as seeding control components, the no-till planter monomer was assembled, and finally prototype trial production and field tests were conducted. Test results showed that the operation efficiency of the no-till planter was significantly improved.

2 Material and methods

2.1 Structure of the seeding machine monomer and working principle

The structure of the high-speed no-till planter monoblock is shown in Figure 1. It consists of a seed box assembly, a fertilizer box assembly, a monoblock frame assembly, a depth wheel assembly, a suppression mechanism assembly, a stubble elimination mechanism assembly, a high-speed seed tube, transmission mechanism assembly, a double-disc furrow opener assembly, and a four-link mechanism assemblies.



1. Seed box assembly 2. Fertilizer box assembly 3. Monoblock assembly 4. Depth wheel assembly 5. Suppression mechanism assembly 6. Assembly of double-disc furrow opener 7. Stubble elimination mechanism assembly 8. Four-link mechanism assembly 9. High-speed seeds 10. Transmission mechanism assembly.

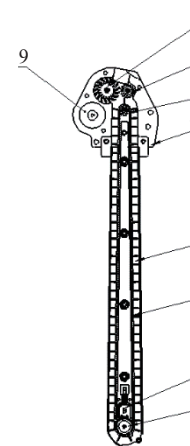
Figure 1 Structural diagram of seeding monomer

A high-speed seed pipe was installed on the seeding monomer of the high-speed no-till planter, and the outlet of the finger clip seed rower was connected with the seed box. The seeds discharged from the finger clip seeder are guided to the outlet of the finger clip seeder and fall along the seed furrow through the high-speed seed pipe. The plant distance is determined by the ratio of the number of teeth of the sprocket on the no-till planter, and the rotation speed of the seeding shaft of the finger clip seeder is changed by the ratio of different sprockets in the transmission system to change the plant distance. The designed seeding monomer can improve the sowing speed of the no-till planter without affecting the plant spacing, row spacing and sowing depth accuracy.

2.2 Design and simulation analysis of high-speed seed tubes

2.2.1 Structural design and working principle

High-speed seed tube is the key component of a high-speed no-till seeding unit, which is the innovative design component of this research. The structure of the high-speed seed tube is shown in Figure 2, which consists of an active feed rubber pulley, a driven feed rubber pulley, an active belt pulley, a gearbox assembly, a lower base plate assembly for the high-speed seed tube, a trapezoidal tooth timing belt, a timing belt tensioning mechanism, a driven belt pulley and a motor.



1. Active feeding rubber wheel 2. Driven feed pulley 3. Master belt 4. Transmission assembly 5. Lower base plate assembly for the high-speed seed tube 6. Trapezoidal tooth timing belt 7. High-speed seed tube tensioning mechanism 8. Driven pulley 9. Motor

Figure 2 Structure of the high-speed seed tube

When the high-speed seed tube is in operation, the seeds fall into the gearbox instantly by the active feeding rubber wheel and the driven feeding rubber wheel into the adjacent two scrapers of the trapezoidal tooth synchronous belt, limiting the space for the corn seeds to move. Then the seeds fall into the seed trench along the direction of the circular arc tangent of the inner wall of the high-speed seed tube. Compared with the current way of common seeds falling freely into the seed trench, the collision and bounce of seeds in the seed tube and the secondary bounce of seeds on the ground were avoided during the high-speed seeding, and the accuracy of spacing and sowing depth was improved. Due to the restriction of the four-link imitation mechanism and the side depth wheel mechanism, the overall design height of the high-speed seed tube should not be greater than 680 mm, the overall breadth should not be greater than 150 mm, and the overall thickness should not be greater than 40 mm.

2.2.2 Trapezoidal timing belt and pulley design

To realize vertical seed conveying and save space, the trapezoidal tooth synchronous belt was selected (Figure 3). There are equally spaced scrapers on the trapezoidal tooth synchronous belt, and the synchronous belt and the bottom plate shell form a plurality of equally spaced seed conveying cavities. The seeds falling from the drop point of the finger clip seed rower enter the seed conveying cavity in turn and are conveyed to the seed furrow by the trapezoidal tooth synchronous belt. Due to the small space of the seed conveying cavity, the seeds would not collide and bounce in the seed guide tube during the falling process, thus the uniformity of the seed falling can be ensured. The diameters of the active and driven pulleys are determined by the linear speed of the belt, and the teeth of the trapezoidal timing belt are meshed with the active and

driven pulleys. The key parameters of the trapezoidal tooth synchronous belt are designed and calculated as follows:

Design power of the synchronous belt drive P_d

$$P = K_A \cdot P_d \tag{1}$$

where, K_A is the load correction factor. P is power transferred, kW. In the previous design, a 795 motor was chosen as the active pulley drive motor, with rated power of 150 W. According to the table, $K_A=1.0$ and $P_d=0.15$ kW.



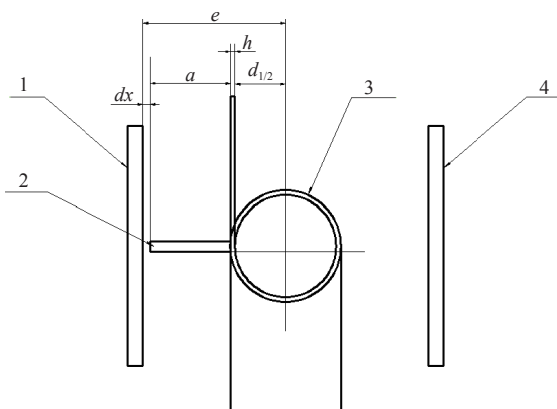
Figure 3 Structural diagram of the trapezoidal tooth synchronous belt

The selection of the synchronous belt should take into account the torque of the pulley at the maximum working speed, the working condition coefficient and the installation space. According to $P_d=150$ W, the maximum speed of the active pulley is 2763 r/min, which calculated according to the operating speed set by the seeder. When the forward speed of the seeder changes, the speed of the high-speed seed tube motor should also change. As shown in the mechanical design selection diagram of the manual synchronous belt, the intersection of power and speed falls in the XL area, so the XL trapezoidal tooth synchronous belt was selected, and its pitch $P_b = 5$ mm^[25].

According to the mechanical design manual specification, the small pulley diameter $Z_1 \leq Z_{min}$ and small pulley tooth number $Z_{min} \leq 12$, followed by consideration of the installation size, the diameter of the active pulley and the length of the trapezoidal tooth synchronous belt, the length of the scraper and the active pulley, high-speed seed tube under the outer wall of the bottom plate shell between the position of the relationship and geometric dimensions, as shown in Figure 4.

$$d_1/2 \leq e - (h + a + \Delta x) \tag{2}$$

where, d_1 is the pitch circle diameter of the active pulley, mm; e is the distance between the center of the pulley and the outer wall of the shell, mm; h is the thickness of the synchronous belt scraper, mm; a is the length of a scraper, mm; Δx is the gap between a scraper and the inner wall of the shell, mm.



1. Left side plate of the lower bottom plate of the high-speed seed tube 2. Scraper finger 3. Driving pulley 4. Right side plate of the lower bottom plate of the high-speed seed tube.

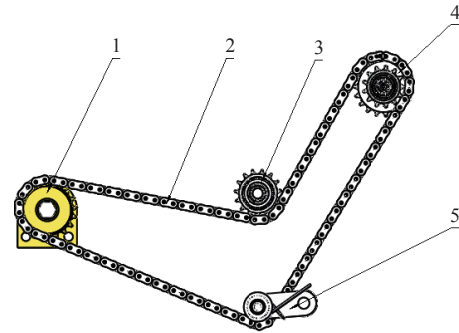
Figure 4 Geometric dimensions of a scraper

It is known that $e=32$ mm, $h=0.8$ mm, $a=16$ mm, and $dx=1$ mm, and $d_1 \leq 28$ mm was obtained. The XL-type synchronous pulley

meets the above conditions and has the close number of teeth of 12, and its joint diameter P_b is 18.9 mm. Set $z_1 = 12$, and then obtain the active pulley joint diameter $d_1 = 19.12$ mm.

2.3 Design of the seeding monomer transmission mechanism

The structure of the transmission mechanism is shown in Figure 5, which consists of a driving sprocket, a 08A chain, a guide sprocket assembly, an outer clutch assembly, and a tension wheel.



1. Driving sprocket 2. 08A chain 3. Guide sprocket assembly 4. Outer clutch assembly 5. Tension wheel

Figure 5 Structural diagram of transmission mechanism

When a single high-speed corn no-tillage seeder carries out seeding operations, the power transmitted by the ground wheel and friction wheel is transferred to the main drive shaft through the transmission system of the no-tillage seeder, and the main drive shaft transfers the power to the driving sprocket of the transmission mechanism in Figure 5 through combination with the sprocket, and the driving sprocket transfers the power and tensions to the outer clutch assembly through combination with the tension wheel. The outer clutch assembly meshes with the seeding shaft on the seed metering device, and the seeding shaft drives the finger clamp seed metering device to sow seeds.

2.4 Simulation analysis on the EDEM-based seed delivery process

2.4.1 Model and parameter determination

The motion law of corn seeds in the high-speed seed tube transport process is complex, and the structural parameters of the high-speed seed tube have a great influence on the delivery effect. The discrete element analysis software EDEM2018 was used to simulate the motion law of maize seeds in the high-speed seed tube and the seed delivery effect.

According to literature, the size of corn seeds is generally 9-13 mm. The software SolidWorks was used to build a three-dimensional model of corn seeds, with length, width and height of 11.3 mm, 9.8 mm and 5 mm, respectively. The model was imported into EDEM to obtain a surface group that matches the outer contour of the three-dimensional model as particles by spherical filling, and a 13 spherical filling was used to build a particle model, as shown in Figure 6. The analysis shows that the trapezoidal tooth synchronous belt trajectory is composed of a straight belt in circular motion, so the structure of the high-speed seed tube model is simplified, as shown in Figure 7. By reviewing literature, the material characteristic parameters and contact characteristic parameters of key components of the corn seed and high-speed seed tube are determined, as listed in Tables 1 and 2^[24].

2.4.2 Simulation analysis on the seed casting process

Through analysis on the seed feeding process of the high-speed seed tube, it can be seen that the shape and angle of the seed feeding plate at the bottom left of the lower bottom plate are the main

factors that affect the seed feeding effect. The design of the seed feeding plate is related to the size of the driven pulley, and two shapes of seed feeding plates were designed according to the actual situation: the seed feeding plate with the combination of circular and linear shapes and the linear seed feeding plate (see Figure 8).

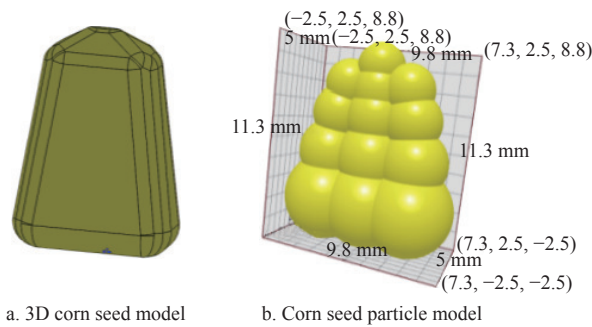
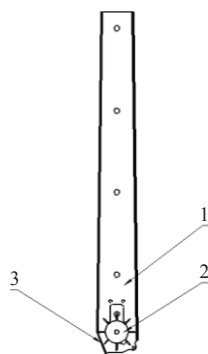


Figure 6 Corn seed model



1. Bottom plate of high-speed seed tube 2. Driven scraper pulley 3. Seed board
Figure 7 Simplified model of a high-speed seed tube

Table 1 Material characteristic parameters of the key components of corn seed and high speed seed tube

Serial number	Characteristic parameters	Corn seed	Polyurethane	Galvanized steel plate
1	Density/g·cm ⁻³	1.197	1.65	2.7
2	Shear modulus/MPa	137	37.68	2700
3	Poisson's ratio	0.40	0.42	0.25

Table 2 Contact parameters of key components of corn seed and high speed seed tube

SerialNo.	Contact parameters	Corn seed-corn seed	Corn seed-polyurethane	Corn seed-galvanized steel plate
1	Static friction coefficient	0.431	0.428	0.351
2	Rolling friction coefficient	0.078	0.085	0.053
3	Crash recovery factor	0.182	0.422	0.709

As shown in Figure 8, for the combined seeding plate, the seeding angle refers to the angle α between the plane of the lower half of the seeding plate and the horizontal line. For the linear seeding plate, the seeding angle refers to the angle β between the plane of the seeding plate and the horizontal direction. The seeding angle needs to be determined according to the direction of seeding and the structure of the high-speed seed tube. The direction of seeding should be opposite to the forward direction of the machine so that the horizontal velocity of the seed row can offset the forward velocity of the machine and improve the quality of seeding. According to the no-till seeder operation requirements, the range of

α is 35°-45°, and β is 68°-74°. In the EDEM simulation analysis, the values of α were set as 35°, 40° and 45°, and β were set as 68°, 71° and 74°, through the simulation results to analyze the influence of the shape and angle of the seeding plate on the qualification index.

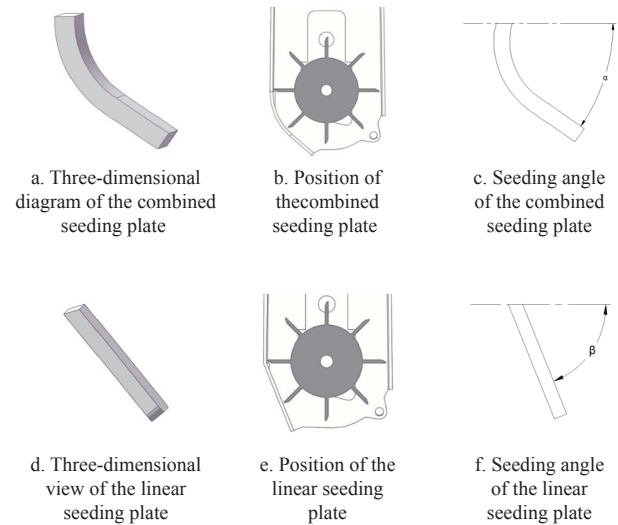
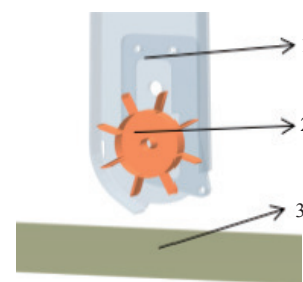


Figure 8 Model diagram of the simulated seeding plate

In the simulation, in order to simulate the motion trajectory of seeds sliding out of the seeding plate, the seeding plate model should be established, as shown in Figure 9. The model mainly includes high-speed seed tube shell, driven scraper pulley and seed bed. The plant spacing was set to 25 cm, the length and width of the seed bed were determined to be 3 m and 30 cm to let the seeds fall smoothly on the seed bed. The seed bed was located directly below the high-speed seed tube, and the center of the seed drop point coincided with the surface center of the seed bed, and the distance between the high-speed seed tube and the seed bed was 30 mm. The test was repeated 10 times. During the simulation, the machine forward speed was 12 km/h, and the plant spacing was 25 cm, and one seed passed every 0.075 s to simulate the actual seeding situation in the high-speed seed tube.



1. Seed tube shell 2. Driven scraper pulley 3. Seed bed
Figure 9 Model diagram of seeding plate

The trajectory of more than one seed on the high-speed seed tube seeding plate is shown in Figure 10. When the corn seeds leave the high-speed seed tube seeding plate, they will contact the seed bed due to their own inertia and certain initial speed, and the corn seeds will keep bouncing up and down on the seed bed and then return to condition of rest after several repetitions. The seed throwing effect of the high-speed seed tube combined seeding plate at 35° is better than the combined seeding plate at 45° and combined seeding plate at 40°, and the seed throwing effect of the high speed seed tube linear seeding plate 74° is better than the linear seeding plate 68° and linear seeding plate at 71°. At the same time,

the seeding effect is better than that of the linear seeding plate at 74° because the seeds come to rest soon after contact with the seed bed.

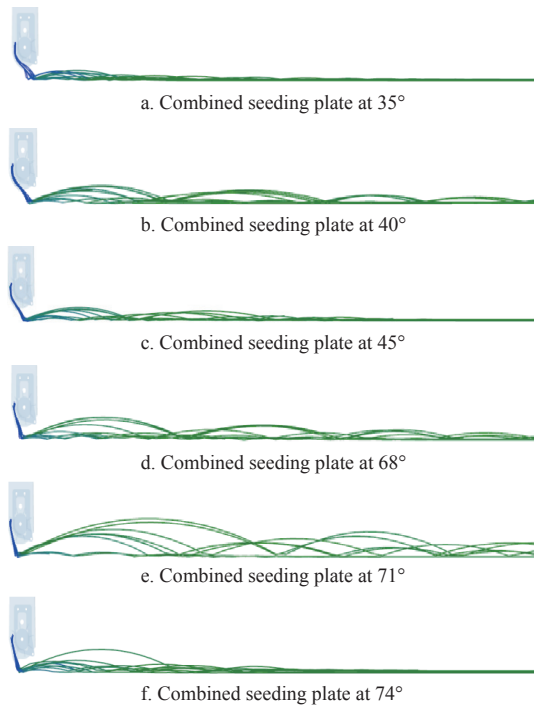


Figure 10 Trajectory of multiple seeds

To quantitatively analyze the grain spacing uniformity, the distance between two seeds was measured using the measurement software, and the data were recorded to calculate the seeding conformity index, which is shown in Table 3. From Table 3, it can be seen that the qualified-seeding index of six seeding plate combinations were ranked as follows: combined seed throwing plate at 35° > combined seed throwing plate at 45° > combined seed throwing plate 40° > linear seed throwing plate 74° > linear seed throwing plate 68° > linear seed throwing plate 71°. The simulation results show that the optimal combination of seeding plate structure parameters is the combination seeding plate with a seeding angle of 35°.

Table 3 Qualified index of seed spacing of combined seeding plates

Serial number	Seeding plate shape	Seeding angle/(°)	Conformity index/%
1	Combination seeding plate	35	95
2		40	86
3		45	83
1	Linear seeding plate	68	82
2		71	83
3		74	87

3 Results and discussion

3.1 Prototyping

A high-speed no-till planter monoblock can operate at a speed of 14 km/h to ensure fixed plant spacing, row spacing and sowing depth. The engineering drawings of the completed high-speed no-till planter monoblock prototype were completed, and machining center was used to process the special parts according to the 3D model, the standard parts such as bearings, trapezoidal gear synchronous belt were selected and purchased, finally, the parts of the machine were assembled, and the production of the high-speed no-till planter monoblock prototype was completed (Figure 11).

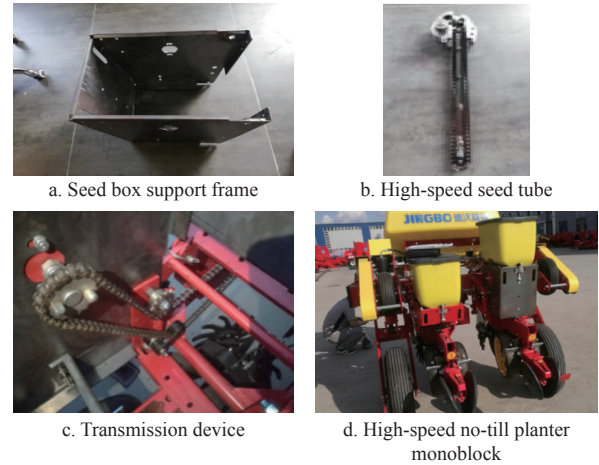


Figure 11 Key components of the high speed no-till planter

3.2 Prototype performance test

The test site was the experimental field of Harbin Swan Lake Farm belonging to Heilongjiang Devo Technology Development Co., Ltd., as shown in Figure 12. The test subjects were selected from Zheng Dan 958 maize seeds with a coating. According to the GB/T6973-2005 single grain (precision) seeder test method and the requirements in the actual operation of a no-till seeder, the qualified-seeding index, multiple-seeding index and miss-seeding index were selected as evaluation indices. The qualified-seeding index can be obtained by calculating the ratio of the number of seeds that meet the requirements of plant spacing and sowing depth to the total number of seeds used in the experiment. The multiple-seeding index can be obtained by calculating the ratio of the number of seeds replanted to the total number of seeds, and the miss-seeding index can be obtained by calculating the ratio of the number of missed seeds to the total number of seeds. According to the design of the test prototype and the bench test, the machine operating speed, the height of the high-speed seed tube from the ground, and the angle of the high-speed seed tube guide were determined as test factors. A single-factor and quadratic regression orthogonal rotation combination test was conducted^[26].



Figure 12 Field test

3.2.1 Single-factor test

(1) Impact of machine operation speed on the evaluation index

According to Figure 13a, the operating speed of the machine had a greater influence on the qualified-seeding index. With the increase in the operating speed of the no-till planter, the qualified-seeding index showed a trend of increase first and then a decrease, and the operating speed reached the maximum value of 95% at 12 km/h. After that, the qualified-seeding index decreased rapidly with increasing operating speed. The effect of the operating speed on multiple-seeding index and miss-seeding index is similar. With the increase in the operating speed of the no-till planter, the change in the qualified-seeding and miss-seeding index at a forward speed of 5-12 km/h was small, with the maximum value of 3, and the minimum value of 2. But when the operating speed continued to increase to 13-14 km/h, due to the performance of the seed planter and the transmission mode of the mechanical chain, the multiple and missing-seeding index of the seed plater increased continuously.

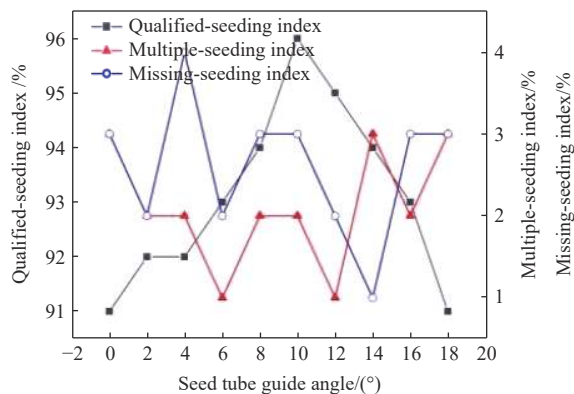
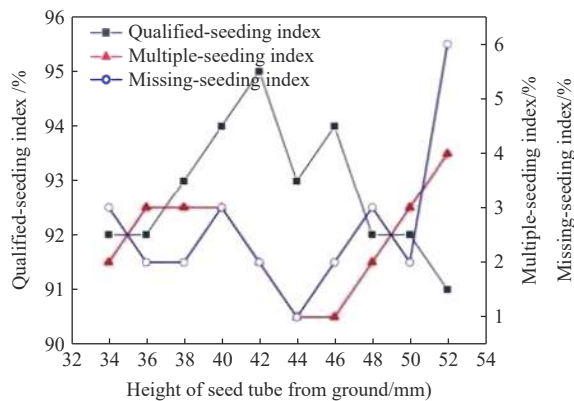
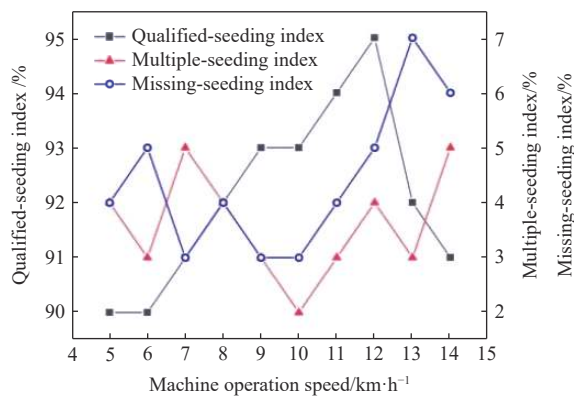


Figure 13 Impact of test factors on evaluation indices

(2) The influence of the height of the high-speed seed tube from the ground on the evaluation index

Figure 13b shows that the influence of the height of the high-

speed seed tube from the ground on the qualified-seeding index is relatively large. When the height of the high-speed seed tube from the ground increased within 34-42 mm, the qualified-seeding index would tend to increase, but with slight change. The height of the high-speed seed tube from the ground 38-42 mm to the maximum value of the qualified-seeding index is 95%. After that, with the increasing height of the high-speed seed tube from the ground, the qualified-seeding index would decrease continuously. The height of the high-speed seed tube from the ground had no effect on the multiple-seeding index and the miss-seeding index with the increase in the height of the high-speed seed tube from the ground, and it can be judged that the multiple-seeding and miss-seeding index had no association with the height of the high-speed seed tube from the ground but with the performance of the seed rower.

(3) Impact of the high-speed seed tube guide angle on the evaluation indices

As shown in Figure 13c, when the machine operating speed and the height of the high-speed seed tube from the ground are certain, the influence of the seed tube guide angle on the qualified-seeding index shows a trend of increase and then a decrease with the increase of the seed tube guide angle, and the seed tube guide angle reached the maximum value of 96% at 10°. The maximum value of the qualified-seeding index was 96% at the time of high-speed seed tube guide angle. After that, with the increase in operating speed, the conformity index of plant spacing decreased continuously. The seed guide angle of the high-speed seed tube had a tendency to change irregularly with the increasing seed guide angle of the high-speed seed tube, so it can be judged that the multiple-seeding and miss-seeding indices are only related to the performance of the seed releaser and not to the guide angle of the high-speed seed tube.

3.2.2 Quadratic regression orthogonal rotation combination test

The results of the single-factor test of the high-speed no-till seed planter were determined with a machine forward speed of 10-14 km/h, seed tube height from the ground of 38-46 mm, seed guide angle of the high-speed seed tube of 7°-11°. The experimental factors were coded as listed in Table 4. The experimental design scheme and results are listed in Table 5.

Table 4 Coding table of sowing test factor level

Code value	Machine advance speed X_1 /km·h ⁻¹	High-speed seed tube height from the ground X_2 /mm	High-speed seed tube seed discharge angle X_3 (°)
-1.682	10	38	7
-1.000	11	40	8
0	12	42	9
+1.000	13	44	10
+1.682	14	46	11

3.2.3 Analysis of the quadratic regression orthogonal rotation combination test results

ANOVA was performed by Design-Expert.V8.0.6.1, and the results of the significance test of the regression equation are listed in Tables 6. The regression models of each test factor and test index were obtained as follows.

(1) Qualified-seeding index Y_1

From the ANOVA results of the qualifying index model in Tables 6, the uniformity model $p < 0.0001$, the model was at a highly significant level, $p = 0.1504 > 0.05$, not significant, and each working parameter in the model was reliable for the evaluation of the seeding qualifying index. The interaction terms of the machine's operating speed (X_1) and the height of the high-speed seed tube from the ground (X_2), the interaction term of the machine's

Table 5 Experimental design and results

Serial number	Test factors			Test results/%		
	X_1	X_2	X_3	Qualified-seeding index Y_1	Multiple-seeding index Y_2	Missing-seeding index Y_3
1	1	1	-1	91	3	6
2	0	0	1.68	89	5	6
3	-1	-1	-1	91	5	4
4	0	0	0	94	3	3
5	-1	1	-1	90	7	3
6	-1.68	0	0	88	8	4
7	1.68	0	0	91	2	7
8	1	-1	1	88	6	6
9	-1	-1	1	87	6	7
10	0	0	0	94	4	2
11	0	0	0	95	2	3
12	0	0	0	94	2	2
13	0	0	0	95	3	2
14	0	0	0	96	3	1
15	0	0	0	96	1	3
16	0	0	0	96	3	1
17	1	1	1	93	2	5
18	0	1.68	0	88	8	4
19	0	0	-1.68	91	4	5
20	0	0	0	94	2	4
21	0	-1.68	0	88	5	7
22	1	-1	-1	90	4	6
23	-1	1	1	86	8	6

operating speed (X_1) and the seed guide angle of the high-speed seed tube (X_3) and the quadratic terms of each factor (X_1^2 , X_2^2 , X_3^2) were significant, while the other terms were insignificant. The order of the three factors affecting the qualified-seeding index was X_1 machine operating speed > X_3 seed tube seed guide angle > X_2 seed tube height above the ground. The regression model after excluding

the insignificant factors was as follows:

$$\hat{Y}_1 = 94.75 + 0.88X_1 - 0.75X_3 + X_1X_2 + X_1X_3 - 1.47X_1^2 - 1.84X_2^2 - 1.34X_3^2 \quad (3)$$

(2) Multiple-seeding index Y_2

The ANOVA results of the multiple-seeding index model in **Tables 6** shows that, the model was at a highly significant level of $p < 0.0001$ for the uniformity model; $p = 0.3265 > 0.05$ for the uniformity model to fit well. Among the terms of the model, the interaction term between the operating speed of the machine and the height of the high-speed seed tube from the ground (X_1X_2) and the quadratic term of each factor (X_1^2 , X_2^2 , X_3^2) were significant. The three factors influenced the multiple-seeding index in descending order: X_1 machine operating speed, X_2 seed tube height from the ground, and X_3 seed tube guide angle. The regression model after excluding the insignificant factors is as follows.

$$\hat{Y}_2 = 2.62 - 1.44X_1 - 1.13X_1X_2 + 0.66X_1^2 + 1.04X_2^2 + 0.54X_3^2 \quad (4)$$

(3) Missing-seeding index Y_3

According to the analysis of variance of the missing-seeding index model in **Tables 6**, it is clear that the model fitting was highly significant ($p < 0.01$) and the out-of-fit term, $p = 0.6049$, which was not significant, indicating that there were no other major factors that affected the index. Among the terms of the model, the interaction terms between the operating speed of the machine (X_1) and the seed tube guide angle (X_3) and the quadratic term of each factor (X_1^2 , X_2^2 , X_3^2) were significant. The order of the three factors affecting the missing-seeding index was X_1 machine operating speed > X_2 seed tube height from the ground > X_3 seed tube seed guide angle. The regression model after excluding the insignificant factors was as follows.

$$\hat{Y}_3 = 2.42 + 0.56X_1 - 0.56X_2 - 0.88X_1X_3 - 0.86X_1^2 - 0.86X_2^2 - 0.86X_3^2 \quad (5)$$

Table 6 Variance analysis of the model

Variance source	Qualified-seeding index Y_1				Multiple-seeding index Y_2				Missing-seeding index Y_3			
	Coefficient	Degree of freedom	F-value	p-value	Coefficient	Degree of freedom	F-value	p-value	Coefficient	Degree of freedom	F-value	p-value
Models	207.27	9	18.17	<0.0001	89.72	9	11.19	<0.0001	70.13	9	8.60	0.0004
X_1	12.25	1	9.67	0.0083	33.06	1	37.11	<0.0001	5.06	1	5.59	0.0344
X_2	1.00	1	0.79	0.3905	1.56	1	1.75	0.2082	5.06	1	5.59	0.0344
X_3	9.00	1	7.10	0.0194	1.56	1	1.75	0.2082	3.06	1	3.38	0.0890
X_1X_2	8.00	1	6.31	0.0260	10.13	1	11.36	0.0050	0.13	1	0.14	0.7163
X_1X_3	8.00	1	6.31	0.0260	0.13	1	0.14	0.7140	6.13	1	6.76	0.0220
X_2X_3	2.00	1	1.58	0.2311	1.13	1	1.26	0.2815	0.13	1	0.14	0.7163
X_1^2	60.36	1	47.63	<0.0001	12.37	1	13.89	0.0025	20.96	1	23.12	0.0003
X_2^2	95.20	1	75.13	<0.0001	30.31	1	34.02	<0.0001	20.96	1	23.12	0.0003
X_3^2	50.50	1	39.85	<0.0001	8.15	1	9.15	0.0098	20.96	1	23.12	0.0003
Residual	16.47	13			11.58	13			11.78	13		
Lack-of-fit	9.58	5	2.23	0.1504	5.36	5	1.38	0.3265	3.78	5	0.76	0.6049
Pure error	6.89	8			6.22	8			8.00	8		
Cor total	223.74	22			101.30	22			81.91	22		

3.2.4 Effect of two factors on test indices

Based on the ANOVA results in **Table 6** and the effect of the one-way test on the passing index, response surface analysis was used to analyze the effect of significant two-way interaction terms on the qualified-seeding index Y_1 , multiple-seeding index Y_2 , and missing-seeding index Y_3 . The results are shown in **Figure 14**.

From **Figure 14a**, it can be seen that when the seed tube guide angle was 9° and the height of the seed tube from the ground was

fixed, with the increase in machine operation speed, the qualified seeding index shows the trend of an increase before a decrease, and the machine operation speed reached the maximum value at 12 km/h. Then the operation speed gradually decreased, because when the machine operation speed increased, the speed of the high-speed seed tube motor changed so that the seed fell along the inner wall of the seed guide tube. The horizontal velocity of the seeds was equal in size and opposite to the forward direction of the machine,

but their velocity along the vertical direction gradually increased, and the seeds would hit the seed furrow due to their shooting speed, and the sowing quality gradually increased. With the increase of the operating speed of the machine, the sowing quality rapidly decreased due to the influence of the performance of the finger clip seed rower. When the operating speed of the machine was fixed, with the increase in the height of the high-speed seed tube from the ground, the sowing depth qualification index also

shows a trend of an increase before a decrease. Because of the lower height of the seed tube from the ground, the seeds on the ground caused by bouncing are also more serious. If the height of the high-speed seed tube from the ground continues to increase, then the seeds would also bounce higher due to free fall. When the machine operating speed was near 0 and the seed tube height from the ground was 0, the qualified-seeding index reached the maximum at this moment.

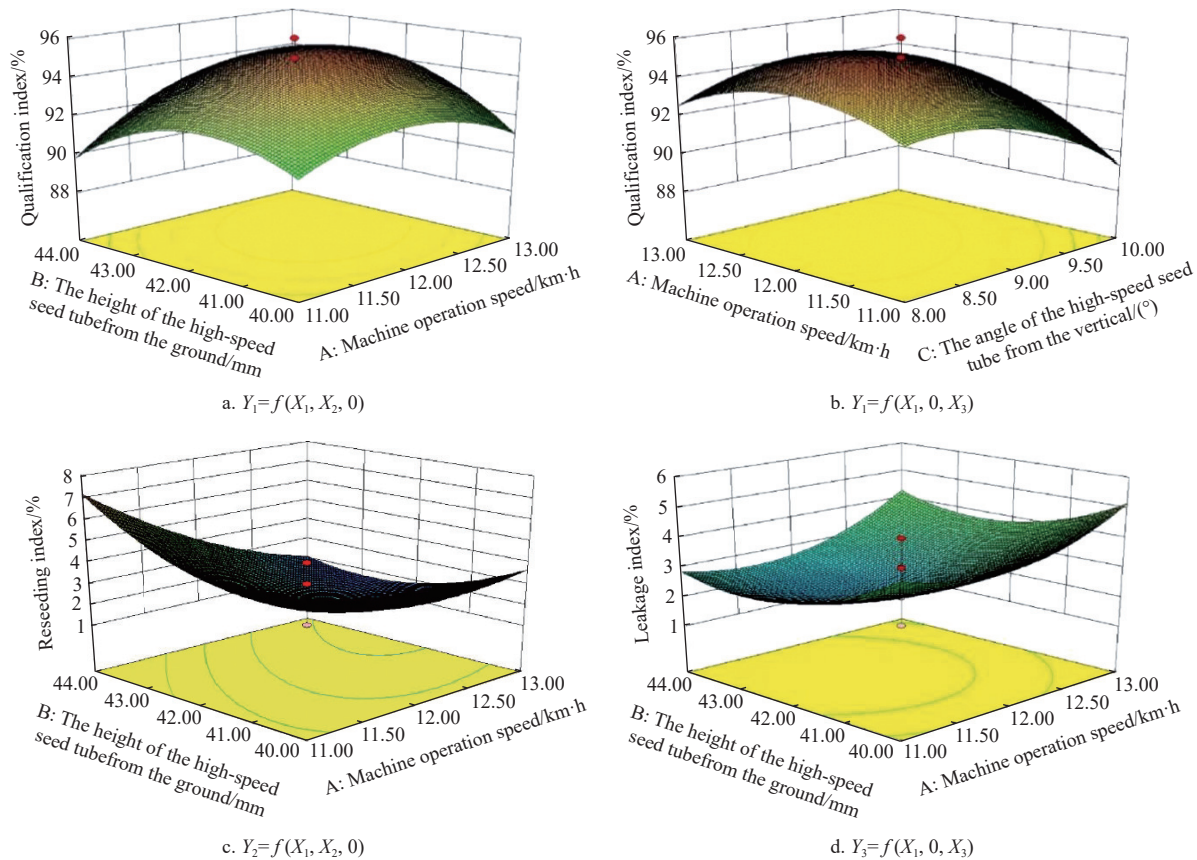


Figure 14 Response surfaces of interaction factors on indices

From Figure 14b, when the height of the high-speed seed tube was 42 mm from the ground, with a fixed operating speed of the high-speed seed tube, the qualified-seeding index increased before a decrease with the change in the seed tube guide angle from the vertical direction of 9° . The reason is that, when the operating speed of the machine was fixed, the seeds were shot out along the wall of the seed guide tube under fixed the motor speed. With the change in the seed guide angle, the seeds were shot out from the high-speed seed tube along the horizontal direction, and the forward speed of the machine gradually approaches each other, so the seeding effect gradually improved. But when the seed guide angle continued to increase, the seeds were shot out along the horizontal direction. However, with the continuous increase of the seed guide angle, the seeds along the horizontal direction and the machine forward speed were not consistent, thus reducing the qualified-seeding index. From the overall point of view, the sowing operation speed and the seed tube guide angle reached the maximum sowing depth qualified-seeding index near the 0 level.

As shown in Figure 14c, when the height of the high-speed seed tube off the ground was kept constant, the multiple-seeding index shows a trend of a sharp increase after a gradual decrease with the increasing forward speed of the machine. The reason is that, the forward speed of the machine would gradually approach

the horizontal directional parting speed of the seed along the outer wall of the seed guide tube with the increase of the operating speed of the machine. The sowing effect gradually improved with the further increase of the performance of the finger clip seed rower, and the probability of multiple-seeding gradually increased.

From the analysis of Figure 14d, when the seed tube guide angle was kept constant, with the increase of the machine forward speed, the missing-seeding index and the multiple-seeding index would show the same trend of gradual decrease before a sharp increase. The reason is that, with the increase of the machine operating speed, the machine forward speed will gradually be close to the horizontal directional parting speed of the seed along the outer wall of the seed guide tube, and the sowing effect would gradually improve. With a further increase in forward speed, the performance of the finger clip seed rower gradually decreased, and the probability of multiple-seeding gradually increased.

3.2.5 Parameter optimization and experimental validation

By taking the qualified-seeding index, multiple-seeding index and missing-seeding index of the particle pitch as the optimization index and using the design-Expert software for optimization analysis, in this test, the qualified-seeding index Y_1 target parameter was maximized, the multiple-seeding index Y_2 target parameter was minimized, the missing-seeding index Y_3 target parameter was

minimized, the upper limit of Y_1 was set to 100, the lower limit was set to 86, the upper limit of Y_2 was set to 8, the lower limit was set to 1, the upper limit of Y_3 was set to 7, and the lower limit was set to 1. The optimization results are as follows: the machine working speed was 12.21 km/h, the height of the high-speed seed tube from ground was 42.23 mm, the high-speed seed tube guide angle was 8.83°, the qualified-seeding index was 94.95%, the multiple-seeding index was 2.33%, and the missing-seeding index was 2.51%.

According to the actual working condition of the machine, the machine was operated at a speed of 12 km/h, the height of the high-speed seed tube from the ground was 42 mm, and the seed tube guide angle was 9°. The test was repeated three times, and obtained an average qualified-seeding index of 94.67%, an average multiple-seeding index of 2.33%, and an average missing-seeding index of 3%. Compared with the results of the quadratic regression orthogonal rotating combination test, the verification test results were similar to the test analysis results, which proved that the single unit of the high-speed no-till seeder met the design requirements.

4 Conclusions

(1) Through the analysis of the development status of no-till sowing machinery at home and abroad, the working principle of advanced high-speed sowing machinery at home and abroad was consulted, combined with the agronomic requirements of corn planting, the overall structural design scheme of the single body of the high-speed no-till planter was determined, and the seed conveying mechanism of the high-speed seed tube was determined to adopt the scraper conveyor mechanism, and the basic size parameters of the high-speed seed tube mechanism were determined. The EDEM discrete element method was used to determine that the bottom seeding plate structure under the high-speed seed tube was a combined seeding plate at a seeding angle of 35°

(2) The prototype of the high-speed no-till planter was completed, and orthogonal rotation combination test and performance test were performed. The optimal working parameter combination of the machine was obtained as follows: the working speed of machine was 12.21 km/h, the height of the high-speed seed tube from the ground was 42.23 mm, and the seed tube guide angle was 8.83°.

(3) This study solved the problem that the inconformity of plant spacing and sowing depth when the operation speed of traditional no-till seeder was higher than 8 km/h and the rotation speed of seed tray was higher than 44 r/min. It is of significance for the research of electrically driven high speed no-till seeders.

Acknowledgements

This study was financially supported by the Liaoning Revitalization Talents Program (Grant No. XLYC2007043), and Scientific Research Fund Project of Liaoning Province (Grant No. LJKZZ20220087) from China Liaoning Province.

[References]

- [1] Zhou J Y. Extension and application of no-till seeding technology for conservation tillage. *Agricultural Development & Equipments*, 2020; 8: 66. (in Chinese)
- [2] Yuan P P, Li H W, Lu C Y, Wang Q J, He J, Huang S H, et al. Design and experiment of seed furrow cleaning device based on throwing and sliding for no-till maize seeding. *Int J Agric & Biol Eng*. 2022; 15(4): 95–102. doi: [10.25165/j.ijabe.20221504.7097](https://doi.org/10.25165/j.ijabe.20221504.7097).
- [3] Karayel D. Performance of a modified precision vacuum seeder for no-till sowing of maize and soybean. *Soil and Tillage Research*, 2009; 104(1): 121–125.
- [4] Cao X P, Wang Q J, Li Hong Wen, He J, Lu C Y, Xu D J, et al. Design and experiment of the pneumatic pressure control device for no-till planter. *Int J Agric & Biol Eng*. 2023; 16(3): 37–46. doi: [10.25165/j.ijabe.20231603.7670](https://doi.org/10.25165/j.ijabe.20231603.7670).
- [5] Lin J, Song Y Q, Li B F. Mechanical no-tillage sowing technology in ridge area of Northeast China. *Transactions of the CSAE*, 2014; 30(9): 50–57. (in Chinese)
- [6] Chen J D, Wang X W, Li H W. Conservation tillage system and no-tillage seeding technology for dryland agriculture. *Journal of Beijing Agricultural Engineering University*, 1993; 13(1): 27–33. (in Chinese)
- [7] Wang P. Current development in maize no-tillage sowing machine and its prospective. *Agricultural Science & Technology and Equipment*, 2012; 3: 73–74. (in Chinese)
- [8] Wang H. Research on 2BMFJ-3 wheat stubble in no-till straw mulching soybean precision seeder. Doctoral dissertation, Northeast Agricultural University. Harbin, China, 2013. (in Chinese)
- [9] Zhang Y F. Analysis of the development status and development trend of seeding machines at home and abroad. *Contemporary Farm Machinery*, 2015; 5: 79–80. (in Chinese)
- [10] She D Q. Research situation of no tillage seeding machine at home and abroad. *Agricultural Engineering*, 2016; 2: 39–40.
- [11] Lin D Z, Hu Z C, Yu Z Y, Gu F W, Wu F, Wu N. Research status and development of straw handling device for no-till seeder. *Jiangsu Agricultural Science*, 2015; 43(11): 13–16. (in Chinese)
- [12] Yang L, He X T, Cui T, Zhang D X, Shi S, Zhang R, et al. Development of mechatronic driving system for seed meters equipped on conventional precision corn planter. *Int J Agric & Biol Eng*, 2015; 8(4): 1–9.
- [13] Sharipov G, Paraforos D, Pulatov A, Griepentrog H. Dynamic performance of a no-till seeding assembly. *Biosystems Engineering*, 2017; 158: 64–75.
- [14] Wang H L, Zhang Z L, Zhang W. Research status and development trend of no-till seeders for mechanized conservation tillage. *Agricultural Mechanization Research*, 2006; 10: 22–24. (in Chinese)
- [15] Wang J H. Current development trend and countermeasures of conservation tillage research. *Agricultural Development and Equipments*, 2018; 1: 67. (in Chinese)
- [16] Liu Y F, Lin J, Hao B Y, Li B F, Ma T. Design and experiment of testing device for soil working tool in no-tillage planter. *Transactions of the CSAE*, 2016; 32(17): 24–31. (in Chinese)
- [17] Liu J Y, Zhang P F, Liu F. Effect of discrete element simulation of seed guide tube height on seed discharge performance. *Agricultural Mechanization Research*, 2016; 38(1): 12–16. (in Chinese)
- [18] Dang Y, Dalal R, Menzies N. Selecting and managing no-till planters and controlled traffic farming in extensive grain production systems. *No-till Farming Systems for Sustainable Agriculture*, Springer, Cham, 2020; pp.83–105.
- [19] Jiang X M. Research on the key technology of precise seeding of corn no-till planter. Doctoral dissertation, Jilin University, Changchun, China, 2017. (in Chinese)
- [20] Zang X G, Wang X Y, Lan H T. Research status and development trend of seeding machinery at home and abroad. *Agricultural Science and Technology and Equipment*, 2014; 12: 53–54. (in Chinese)
- [21] Li H W, Chen J D, Deng J, Zhao W. Study on technology and machines of mechanized conservation tillage for dryland maize. *Journal of China Agricultural University*, 2000; 5(4): 68–72. (in Chinese)
- [22] Chen C. Structural design and performance test research of belt-type seed guide device for precision seeder. Doctoral dissertation, Inner Mongolia Agricultural University, Huhehaote, China, 2016. (in Chinese)
- [23] Shi S. Design and experimental research on pneumatic combination hole type corn precision seed discharger. Doctoral dissertation, China Agricultural University, Beijing, China, 2015. (in Chinese)
- [24] Liu Q W. Design and experimental research on precise seed feeding mechanism of high-speed seeder. Doctoral dissertation, China Agricultural University, Beijing, China, 2017. (in Chinese)
- [25] Wen B C. Machine design handbook. China Machine Press, Beijing, China, 2010. (in Chinese)
- [26] Liu Y X, Shang S Q, Wang D W, Cui Z C, Yang H G. Design and experiment of inclined inserted no-tillage hill seeder. *Transactions of the CSAE*, 2017; 33(23): 8–14. (in English)